MICROWAVE REFLECTION MEASUREMENTS OF ELECTRON DENSITIES IN ELECTROMAGNETICALLY DRIVEN SHOCK PRODUCED PLASMAS

AKIMASA FUNAHASHI and SUSUMU TAKEDA

Department of Electrical Engineering

(Received October, 1967)

Abstract

The electron densities from 10^{13} to 10^{17} cm^{-3} in plasmas produced by electromagnetically driven, propagating or reflected shock waves are measured by a microwave reflection method. The Mach number of the shock waves is varied from 9 to 25 in gases at pressures from 0.4 to 2.0 mmHg. The gases used are argon, air, helium and hydrogen. A 35-Gc microwave reflection probe is inserted into a T-type shock tube perpendicular to its axis, or is placed at the tube end parallel with the axis. Even though some perturbation on the gas flow by the inserted probe is expected, surprisingly good agreements are found between the microwave and spectroscopic measurements. Moreover, no difference is observed between the electron densities measured from the spectral line broadening for the cases with and without the inserted probe. This means that the electron densities are not much disturbed by the inserted probe. Such measured electron densities are compared with theoretically predicted values which are calculated from the Rankine-Hugoniot and Saha equations.

For Mach numbers higher than 20, the maximum values of the electron densities measured behind the shock fronts agree well with the theoretically predicted values. For low Mach numbers, however, the measured maximum electron densities are lower than the theoretically predicted values. The discrepancy between the measured and theoretical densities, which increases with decreasing Mach number and initial gas pressure, may be due to the long relaxation time and an insufficient thermal equilibrium behind the shock front. The measured build-up time of the electron density behind the shock front also increases with decreasing Mach number and initial gas pressure.

I. Introduction

Recently much attention has been paid to plasmas produced by shock waves in order to study magnetohydrodynamics, re-entry physics and problems on flights of hypersonic vehicles and to produce high density plasmas for controlled thermonuclear fusion research[1]. It is the purpose of this report to investigate whether or not the measured plasma densities agree with theoretical values calculated from the Rankine-Hugoniot equations and Saha's equation. This last equation assumes thermal equilibrium. In a conventional pressure driven shock tube, the measured densities almost agree with the theoretical predictions[1]. Tevelow[2] has reported a good agreement in shocked air. However, comparisons of the experiment and the theory are not well studied in an electromagnetically driven shock tube.

The plasmas produced by shock waves have been mainly studied by the spectroscopic method in a conventional pressure driven[3] and electromagnetically

driven[4)-6)] shock tube. The densities and temperatures measured immediately behind shock fronts in a T-tube have shown an agreement, within a factor 2 or 3, with the theoretically predicted values for Mach numbers higher than 25 in hydrogen or helium at initial pressures of a few mmHg[5)]. Some discrepancy between the experiment and shock theory has been explained by a radiative energy transfer from the initial arc discharge into the gas ahead of the shock front[5)]. In these experiments the electron densities and temperatures have been higher than 10^{17} cm^{-3} and a few eV respectively. However, it is difficult to measure the electron densities in the range from 10^{14} to 10^{16} cm^{-3} by means of the spectroscopic method, since the method appears to work only at sufficiently high electron densities. The conventional optical interferometer[6)7)] is not applicable to low electron densities produced by shock waves of relatively low Mach number. The microwave transmission technique can not be also applied to plasmas of electron density higher than 10^{14} cm^{-3} even with a microwave of 100-Gc[8)]. Thus, the investigations of the plasmas produced by the shock waves of relatively low Mach number in a pressure range of a few mmHg have not been reported except for a few cases[9)]. The Langmuir probe technique may not be reliable enough for fast, time varying, or non-reproducible plasmas, and the error would be significant[10)] when some fraction of the discharge current flows to the probe in an electromagnetically driven shock tube.

A microwave reflection method, which was proposed by one of the authors[11)], has some advantages: (1) a wide range of the electron density higher than the cut-off density can be measured with a single microwave frequency, and (2) the electron density and the collision frequency, which are related to a complex reflection coefficient of a microwave at a sharp plasma boundary, are easily determined from the amplitudes of the standing wave at two proper positions. The method was first applied to an afterglow plasma in a waveguide[12)] and then to plasmas which were produced by shock waves reflected at the end wall of a shock tube in a waveguide[13)].

As a natural extension of the microwave reflection method to cover wide experimental conditions, a microwave reflection probe[14)] was developed to apply the method to plasmas in free space with a reasonable spatial resolution. The microwave reflection probe has been used for measurements of a magnetically confined arc[15)] in a steady state and of plasmas produced by reflected shock waves[16)]. The microwave reflection probe is different in principle from that used by Lin *et al.*[25)] who measured the reflected power from plasmas of electron density lower than the cut-off density.

Meanwhile, the electron densities and the collision frequencies in plasmas behind propagating shock waves have been determined by Brandewie and Williams[17)] from the measured complex reflection coefficient of a microwave at the plasma behind the shock front. The plasma has been assumed to have the electron density distribution of a hyperbolic tangent form along the tube axis. With this electron density distribution, the calculations are extremely complicated. The incident microwave, however, has been reflected mainly at the ramp of the electron density behind the shock front and has not reached the part of the maximum electron density unless the penetration depth of the microwave has been deeper than the characteristic width of the electron density ramp. In fact, the penetration depth[8)11)] is very shallow, that is, approximately 0.5 mm for the

electron density of 10^{14} cm^{-3} and 0.05 mm for 10^{16} cm^{-3}, while the measured ramp widths are about a few cm (depending on the shock velocity). Thus, the reflection coefficient of the microwave would not have been affected significantly by the maximum electron density. The measured electron densities and collision frequencies in the reference (17) may not be reliable enough. The thickness of the sheath, which is inevitably formed at the boundary between the plasma and the microwave reflection probe, is much thinner[11] than the penetration depth in most cases[20]. Thus, the effect of a non-uniform electron density in the sheath can be perfectly neglected in calculating the reflection coefficient at the plasma boundary in the present method.

Bethke and Ruess[18] have determined only the collision frequencies in plasmas produced by pressure driven, propagating shock waves from the measured reflected powers of a microwave, where the axial electron density distribution has been assumed to be an exponential form.

In the previous work[13], a shock tube has been inserted into a 9-Gc circular waveguide having an inner diameter equal to the outer diameter of the shock tube. The electron densities have been measured in plasmas produced by reflected shock waves in this tube. In the present work, a 35-Gc microwave reflection probe is perpendicularly inserted into a shock tube in order to avoid the complicated effect due to the axial electron density distribution behind propagating shock fronts. In addition, another type of 35-Gc microwave reflection probe is placed at the shock tube end in parallel with the axis and is used to measure the electron densities in plasmas produced by reflected shock waves.

On the other hand, the Stark broadening of the spectral line is also used to measure the electron densities. Measurements are made of Mach numbers from 9 to 25 at pressures of a few mmHg. The measured electron densities are compared with the theoretically predicted values, which are calculated from the Rankine-Hugoniot and Saha equations by using the measured shock velocity and the initial gas pressure. The theoretical considerations neglect the complicated effect due to the precursor, various loss processes and the relaxation phenomena behind the shock fronts.

Some preliminary results have been previously published elsewhere.[16][19]

II. Experimental Apparatus

A *T*-type shock tube, which is made of Pyrex glass and has an inner diameter of 2.2 cm and a length of about 67 cm, is filled with various gases at pressures of a few mmHg. The gases used in the experiments are argon, air, helium and hydrogen. The shock waves are produced by discharging through an air gap switch four capacitors, each of which has 4 microfarad and can be charged up to 15 KV. The ringing frequency and the maximum current of the discharge are approximately 90-Kc and 10^5 ampere respectively. The microwave reflection probe is inserted perpendicularly into the shock tube at the position 50 cm away from the electrodes in the case of propagating shock wave experiments, and is faced to the shock tube end in the case of reflected shock wave experiments. The luminous front of the shock wave is monitored by two light pipes which lead to two photomultipliers. The shock velocity is, then, obtained as the ratio of the separation distance L between these two light pipes to the time interval

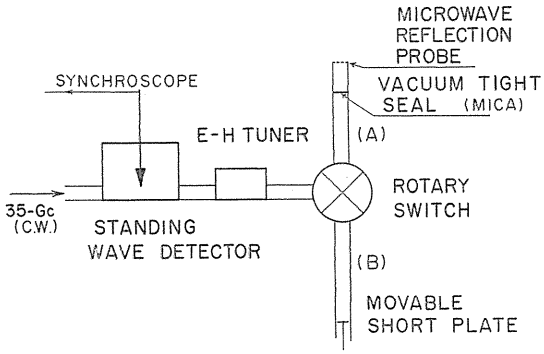

FIG. 1. Schematic diagram of the microwave circuit.

between observed discontinuous photomultiplier signals.

In Fig. 1 is shown the schematic diagram of the measuring microwave circuit. The 35-Gc cw microwave from a klystron is supplied through a rotary switch to either the measurement arm with the microwave reflection probe or the reference arm with a movable short plate. The position of the movable short plate is pre-adjusted so that both arms have the same effective lengths. The E-H tuner is used to eliminate a reflection at the probe end, when no plasma exists outside the probe[14]. The correct position of the standing wave detector, which will be described in the next section, is found by turning the rotary switch to the reference arm: the movable short plate is substituted for the plasma of infinite electron density. Next turning the rotary switch to the measurement arm, the output signals of the standing wave detector for plasmas are displayed on the synchroscope.

The microwave reflection probe consists of a piece of 35-Gc standard rectangular waveguide. When the probe is perpendicularly inserted into the shock tube, the construction is shown in Fig. 2 (a). The waveguide is covered with a glass tube in order to be electrically isolated from the plasma. On the probe end is attached a very thin mica plate. Then a sharp discontinuity of electron density is realized just outside the probe. The distance of the probe end from the shock tube wall is about 5 mm. In Fig. 2 (b) the microwave reflection probe is attached to the end wall of the shock tube. The probe has a glass window of 1/4 wavelength thickness at its end. Such a dielectric window makes it possible to measure sensitively high electron densities[20][21]. The effect of the dielectric window is described in Section III.

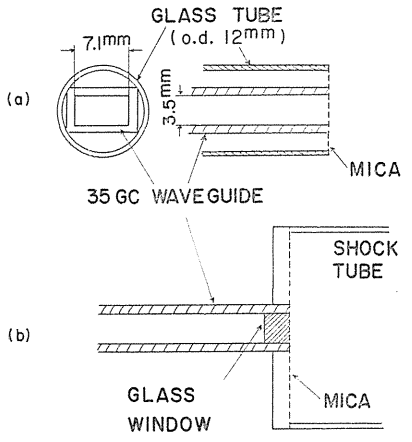

FIG. 2. Construction of the 35-Gc microwave reflection probe for propagating (a) and reflected (b) shock wave experiments.

III. Principle of the Measurement

Since a detailed description of the present method has been already published[13)20)], only the principle is described here briefly. The principle is based on the fact that the complex reflection coefficient of a microwave at a sharp plasma boundary depends on the electron density n and the electron collision frequency ν of the plasma. Such a sharp plasma boundary is realized at the probe end.

The complex reflection coefficient can be then deduced from two standing wave signals, h_3 and h_4, observed at positions effectively $\frac{1}{8}\lambda_g$ and $\frac{3}{8}\lambda_g$ distant from the probe end respectively. Thus, the values of h_3 and h_4 are just one half of the standing wave maximum for the plasma of infinite electron density. Using Δh_3 and Δh_4 which are the differences between the values of h_3 and h_4 for a finite electron density to be measured and those for a metal short plate at the probe end, one obtains the following equations, provided that $\eta \gg 1+\delta^2$,[16)20)]

$$\eta = \frac{1}{\Delta h_3 \cdot \Delta h_4} \tag{1a}$$

$$\delta = \frac{\Delta h_4^2 - \Delta h_3^2}{2\,\Delta h_3 \cdot \Delta h_4} \tag{1b}$$

where Δh_3 and Δh_4 are normalized to unity by the maximum of the standing wave for perfect reflection. η and δ are the normalized electron density and collision frequency respectively and defined here as,

$$\eta\left(\frac{\lambda}{\lambda_g}\right)^2 \equiv \frac{\omega_p^2}{\omega^2} = \frac{4\pi n e^2}{m_e \omega^2}$$
$$\delta \equiv \frac{\nu}{\omega} \tag{2}$$

where e and m_e are the charge and mass of the electron, ω_p and ω are the plasma and applied microwave angular frequencies, λ and λ_g are wavelengths in free space and in the waveguide respectively, and $\left(\frac{\lambda}{\lambda_g}\right)^2$ is the correction factor for the guided wave propagation.

Equation (1) simplifies to

$$\eta = \frac{1}{\Delta h_4^2} \tag{3}$$

for $\delta^2 \ll 1$. More generally the following equation is deduced,

$$\frac{\eta^2}{\eta - 1} = \frac{1}{\Delta h_4^2} \tag{4}$$

for $\eta > 1$ and $\delta^2 \ll 1$.

When the collision frequency is small compared with the applied microwave angular frequency, the electron density can be determined in an extremely simple way from Eq. (3) or (4).

The small differences in the phase angle of a reflection coefficients can be expanded by using a dielectric plate of 1/4 wavelength thickness[20)21)]. This results

that, when η is extremely high, one can measure the high electron density very accurately with a microwave reflection probe as shown in Fig. 2 (b). For the probe with the dielectric window, one can obtain the following equations corresponding to Eqs. (1 a), (3) and (4),

$$\eta = \frac{\varepsilon^2}{\Delta h_3 \cdot \Delta h_4} \tag{5}$$

for $\eta \gg \varepsilon^2\sqrt{1+\delta^2}$,

$$\eta = \frac{\varepsilon^2}{\Delta h_4^2} \tag{6}$$

for $\eta \gg \varepsilon^2$ and $\delta^2 \ll 1$, and

$$\frac{(\eta - 1 + \varepsilon^2)^2}{\eta - 1} = \frac{\varepsilon^2}{\Delta h_4^2} \tag{7}$$

for $\eta < 1$ and $\delta^2 \ll 1$. Here ε is the specific permitivity of the dielectric plate. The expression for δ is same as Eq. (1 b).

IV. Effect of the Fringing Field

Since the guided wave propagation is no longer valid just outside the probe end, the effect of the fringing field on the penetration depth has to be taken into account. In a previous paper[14], an heuristic and semi-emperical method was developed in order to evaluate the fringing field effect.

η' is regarded as an apparent normalized electron density which is slightly different from the true density η because of the fringing field effect. In order to obtain the relation between η' and η a decaying plasma ($\delta^2 \ll 1$) is used which is realized in the vicinity of the end wall of a shock tube after the shock wave is reflected there. Two pieces of 35-Gc standard rectangular waveguide are attached normally to the end wall of a shock tube whose inner diameter is 5.0 cm, as is shown in Fig. 3. The end of the waveguide (A) is in the same plane of the inner surface of the shock tube end wall, while the waveguide (B) is pulled out by some distance in such a way that the hole in the end wall behaves like a short waveguide connected smoothly to the waveguide (B). On both ends of the waveguide (A) and (B) are attached very thin mica plates. Thus the apparent value of η, η', obtained at (A) includes the fringing field effect, whereas the value of η obtained at (B) is considered to correspond to the real electron density without the fringing field effect. Because the penetration depth is shallower than the relative displacement of about 4 mm between the two waveguide ends, the electron density outside the waveguide remains the same for (A) and (B),

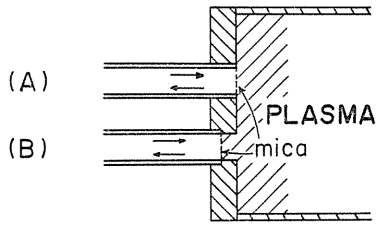

FIG. 3. Effect of the fringing field on the microwave reflection probe.

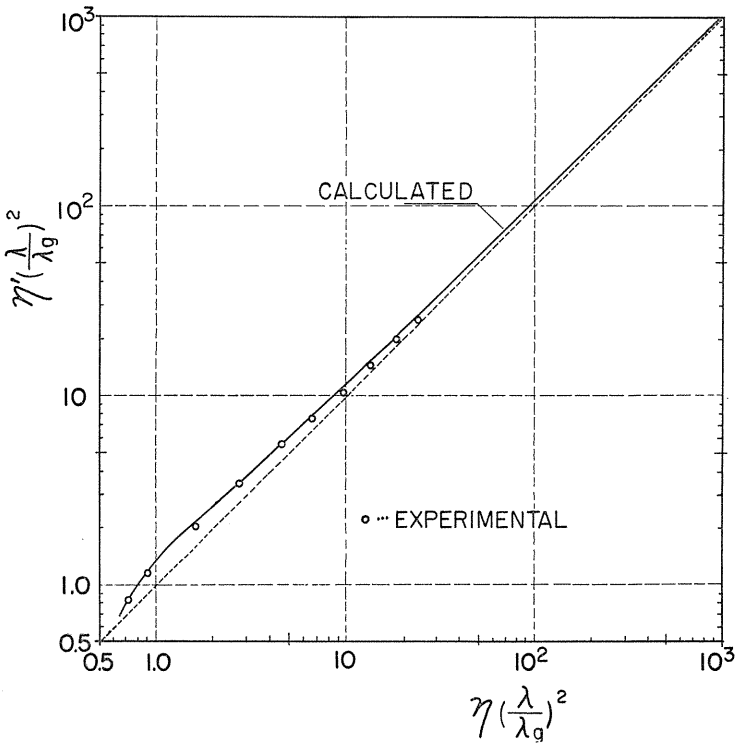

FIG. 4. Relation between $\eta'\left(\frac{\lambda}{\lambda_g}\right)^2$ and $\eta\left(\frac{\lambda}{\lambda_g}\right)^2$.

The values of η' and η determined from Eq. (4) are compared in Fig. 4, where η' and η are multiplied by $\left(\frac{\lambda}{\lambda_g}\right)^2$ as a correction for the guided wave propagation. The solid line is calculated from an experimental formula previously described.[14] As is physically expected, the correction for the fringing field effect decreases rapidly with increasing η: it is less than 15 percent for $\eta\left(\frac{\lambda}{\lambda_g}\right)^2 > 20$ as is seen in Fig. 4. The probe shown in Fig. 2 (a) has no flange, while the waveguide (A) in Fig. 3 has a flange of the end wall. The effect of the flange, however, would not be serious.

The experiment is extended to the probe which has a dielectric window of 1/4 wavelength thickness and is shown in Fig. 2 (b). A glass plate, which is used as the dielectric window, has an effective specific permittivity of 9.65 in the waveguide. In Fig. 5 are shown the time variations of electron densities measured by both the probe with the glass window and a thin mica window (negligible thickness). The curve a is plotted for the probe with the mica window, where the low density is corrected by the curve in Fig. 4. The curve b is plotted for the probe with the glass window. It should be noticed that the E-H tuner is not used for the latter probe, because the matching process almost cancels the expansion effect in the phase angle by the glass window[22]. Thus, the electron density higher than 10^{15} cm^{-3} can be sensitively measured by the probe with the

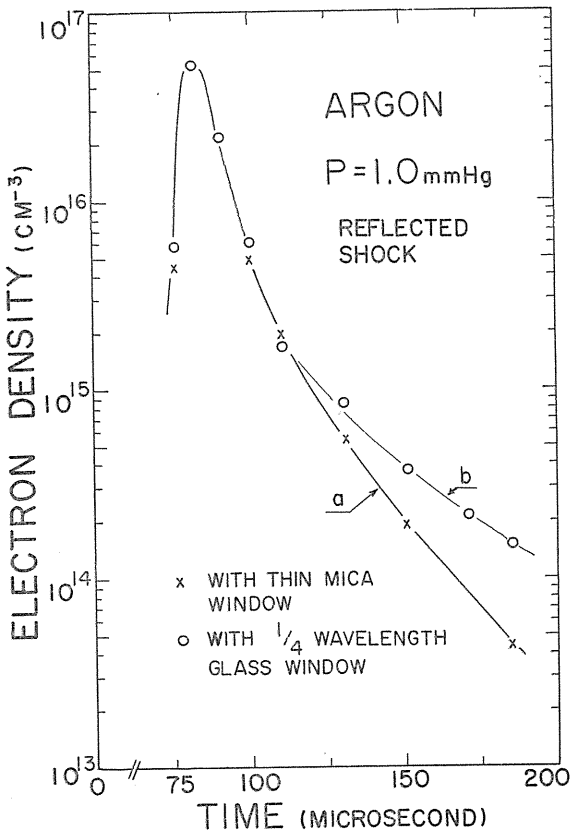

FIG. 5. Comparison of the electron density measured with the probe with the glass and the mica window. (the origin of the time is the initiation of the discharge in the shock tube).

glass window.

Hermansdorfer[23] has measured spatial and time density variations in a linearly pinched plasma with a 35-Gc microwave reflection probe with a dielectric window. However, since the fringing field effect has not been taken into account, the measured low densities include appreciable errors.

V. Experimental Results

1. Relation between electron density and Mach number

In Fig. 6 is shown a typical example of the observed h_4 signals and shock velocities for propagating (incident) shock waves in argon. The maximum value of the h_4 signal, and the time T for the shock wave to propagate the distance L between the two light pipes are plotted versus the time T_0 required for the shock wave to arrive at the observation position. Each maximum value of h_4 corresponds to the maximum electron density behind a shock front. The height h_4' is obtained for a metal plate at the probe end, as described in Section III. Then $\Delta h_4 \equiv h_4' - h_4$

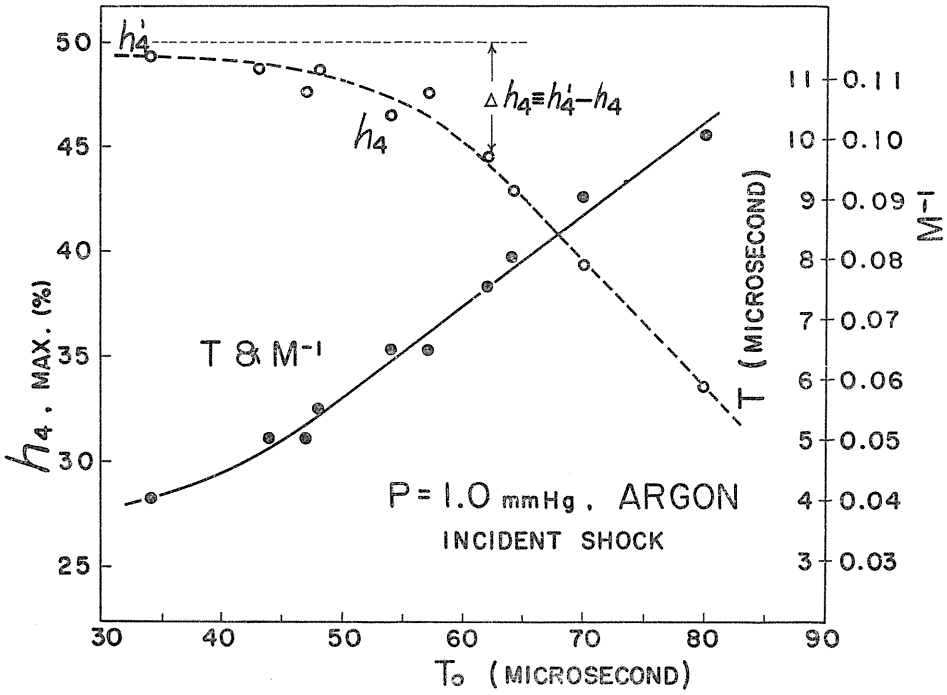

FIG. 6. Maximum value of h_4, the time T for the shock wave to propagate the distance between two light pipes, and Mach number M versus the arrival time T_0 at the observation position.

can be easily determined from a smooth curve which is drawn through the scattered points of the observed h_4 signals. The h_3 signals are also observed. Each value of η is calculated from the Δh_4 and Δh_3 by Eq. (1 a) for $\eta \gg 1+\delta^2$, and by Eq. (3) or (4) for $\delta^2 \ll 1$. The value of η is corrected by the curve shown in Fig. 4 when η is low. The electron densities are then deduced from Eq. (2). The Mach number M in Fig. 6, is calculated from T and L. However, it is more accurate to determine the Mach number from the observed T_0, by using a smooth curve which is drawn through the scattered points of T and M^{-1} versus T_0, as is shown in Fig. 6.

In Fig. 7 (a) and (b) are shown the measured maximum electron densities versus the Mach numbers in argon at initial pressures of $p=1.0$ mmHg and 0.5 mmHg respectively. In Fig. 7 (b) are also shown the electron densities measured by McLaren *et al.*[9], who have used a double probe in a shock tube apparatus similar to that reported here. Their measured low densities seem to coincide with ours within an experimental error. The measured maximum electron densities are shown in Fig. 8 for two different initial pressures in air. In this figure are also shown the measured values determined from the microwave cut-off. Thus, the measured densities are considered to be reliable enough, at least, for low Mach numbers.

The error bars of the measured electron densities indicated in Figs. 7 and 8

are evaluated by assuming that the error in h_3' and h_4' is within 1 percent. The solid curves in Figs. 7 (a) and (b) are theoretically calculated from the Rankine-Hugoniot and Saha equations for argon[1)24)]. In these numerical calculations, second ionization and the excitation energy are neglected in the enthalpy equation. The theoretical values in Fig. 8 are estimated from the theoretical densities at an initial pressure of 0.02 mmHg, since the maximum densities are almost proportional to the initial gas pressure[25)]. The measured electron densities are much lower than the theoretically calculated ones for relatively low Mach numbers, and the measured values fairly agree with the theoretical ones for Mach nnmbers higher than 20.

In order to confirm a reliability of the present method at high densities, the Stark broadening technique is used to determine the electron density. Measurements are made in helium for both propagating and reflected shock waves, where the *HeI* (4471 Å) line is used. The eight suitable wavelengths within the line profile are chosen by a grating monochrometer on successive discharges. A photomultiplier (1 P 21) which is focused at the observation position through a light pipe is used to observe the relative intensities at these wavelengths. Thus

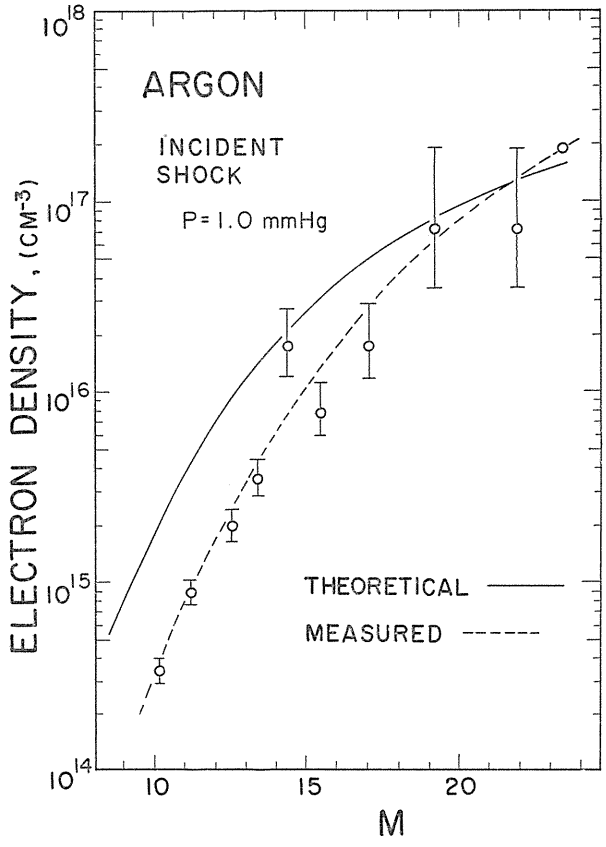

FIG. 7 (a)

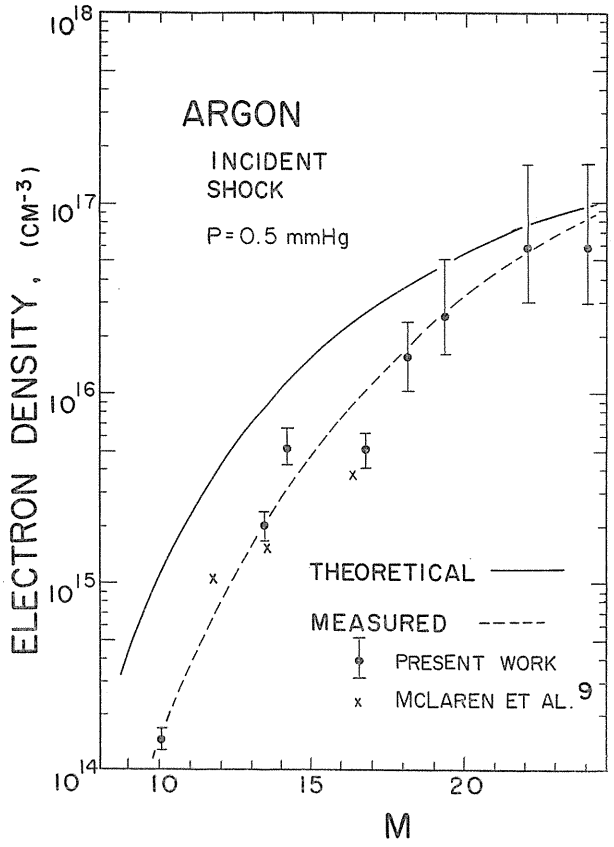

FIG. 7 (b)

FIG. 7. Maximum electron density behind the propagating shock wave versus Mach number in argon.
(a) initial pressure, $p=1.0$ mmHg.
(b) $p=0.5$ mmHg.

the electron density is determined from the half-width obtained from the measured line profile[26)27)].

The results measured at two different initial pressures are shown in Figs. 9 (a) and (b) for propagating and reflected shock waves respectively. In these figures the theoretically calculated densities (solid line) are also shown to compare with the measured densities (dotted line) with the microwave reflection probe (M. R. PROBE). The accuracy in the measured densities is improved in Fig. 9 (b), because the sensitive probe with the glass window is used in this experiment.

The electron densities measured from Stark broadening for $M\simeq 19.5$ at initial pressure $p=0.4$ mmHg and for $M\simeq 15.5$ at $p=2.0$ mmHg are respectively compared in Fig. 9 (a) for both cases with the probe inside the shock tube and without it. Both values show a surprising good agreement, even though a considerable disturbance is expected on the gas flow by the existence of the probe. This

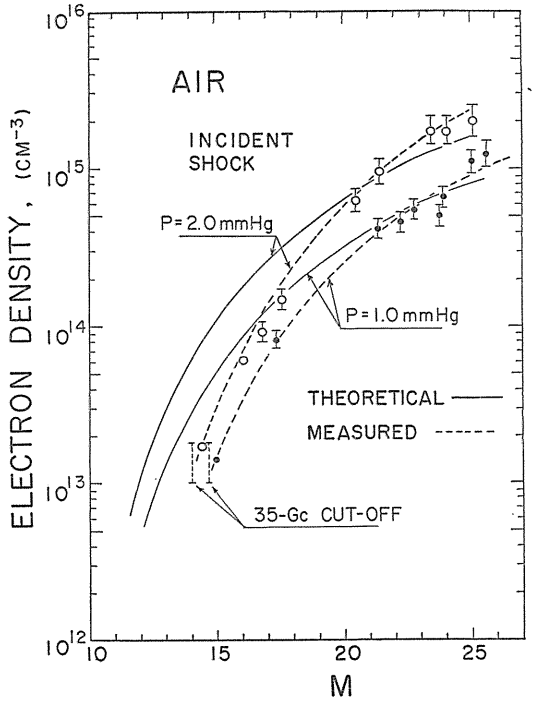

FIG. 8. Maximum electron density behind the propagating shock wave versus Mach number in air.

means that the plasma produced by the shock wave immediately recovers the original state, suppressing the disturbed layer close to the probe. When a propagating shock wave arrives at the shock tube end and reflects there (see Fig. 2 (b)), a sharp boundary of plasma is established just outside the probe end. Then the increased electron density behind the reflected shock wave covers the range from 10^{16} to 10^{17} cm^{-3}. For the plasma, both methods: Stark broadening and microwave reflection probe can be used in the same experimental conditions. A satisfactory agreement is found between the electron densities measured by both methods, as is shown in Fig. 9 (b). Since no disturbance is produced by the probe, which is not inserted into the shock tube as shown in Fig. 2 (b), the discrepancy between the measured and theoretically calculated values is significant in this experiment.

2. Electron densities behind shock fronts

(i) Propagating shock waves

The change of the electron density along the shock tube axis can be determined by analyzing the shape of the observed h_3 and h_4 signals. Figure 10 shows an example of the axial distribution of electron density thus measured for different Mach numbers in argon[19]. The origin of the time is not the shock front, but the luminous front which is determined from the discontinuity of the photomultiplier signal at the observation position. The space resolution of the probe

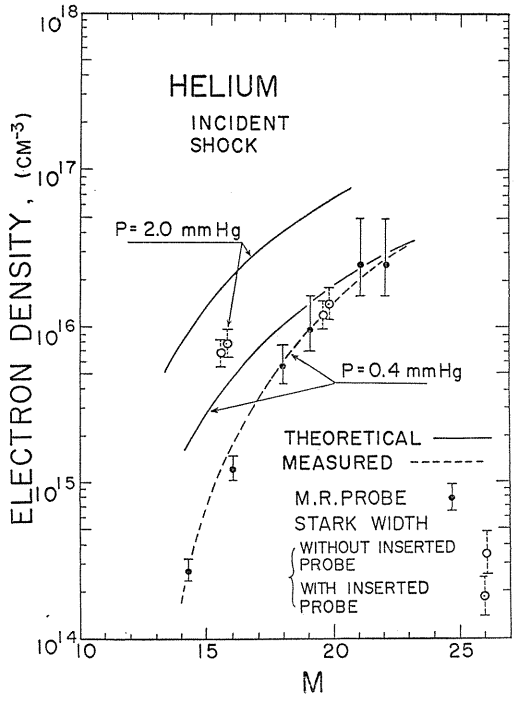

(a)

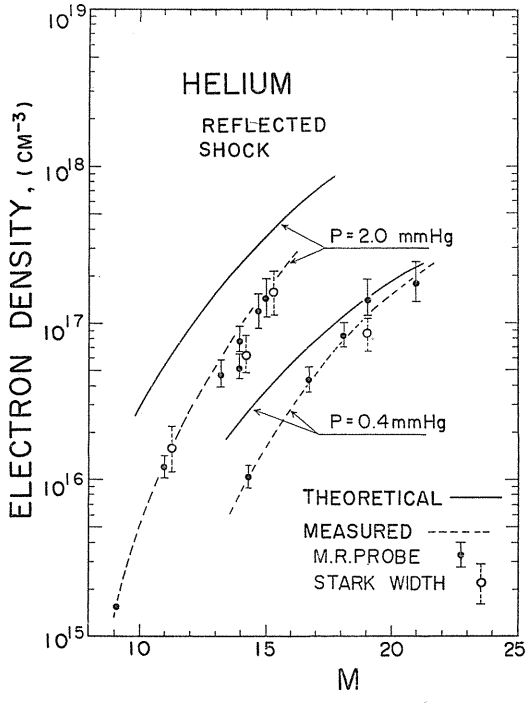

(b)

FIG. 9. Maximum electron density versus Mach number at different initial pressures in helium.
(a) propagating shock wave.
(b) reflected shock wave.

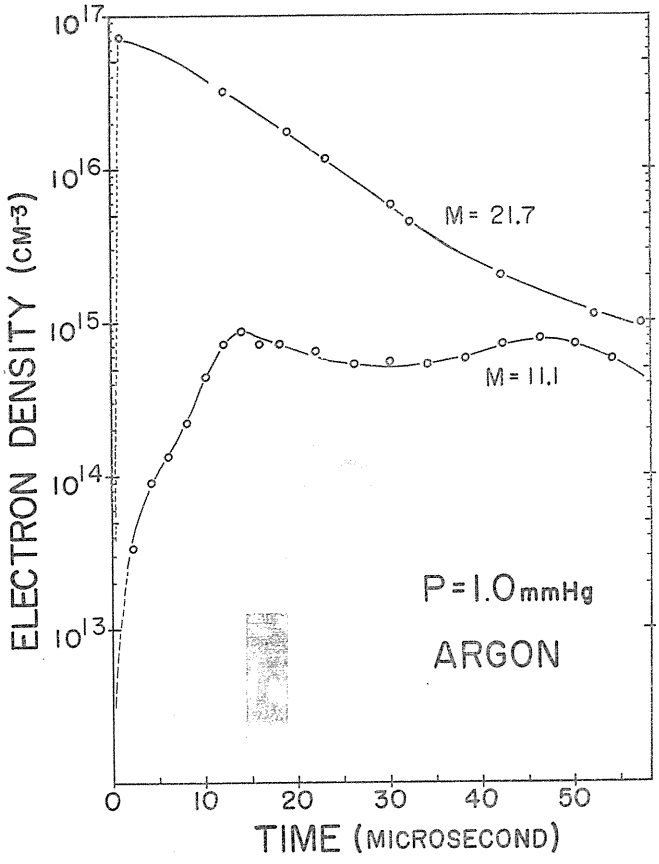

FIG. 10. Axial electron density distributions for different Mach numbers.

along the shock tube axis is about equal to the size of the waveguide. Thus, the probe has a time resolution equal to the space resolution divided by the shock velocity, that is, about 1.0 microsecond for the propagating shock wave whose Mach number is 20 in argon.

It is seen from Fig. 10 that the electron density behind the shock front builds up more slowly at the lower Mach number than at the higher Mach number. For example, the electron density attains its maximum value at about 15 microseconds after the arrival of the luminous front for $M=11.1$ in argon at a pressure of 1.0 mmHg, and the corresponding width of the axial electron density gradient of the plasma is about 5.3 cm. For $M=21.7$, on the other hand, the electron density builds up more quickly than the time resolution of the probe. Two peaks of the measured axial electron density profiles at $M=11.1$ are considered to correspond to the plasma produced by the shock wave and following driver arc plasma. At $M=21.7$ no separation between these two plasmas is observed. It is well-known that two plasmas which are observed separately at relatively low Mach numbers coincide with each other at higher Mach numbers[28].

The build-up time τ which is defined here as the time for the electron density

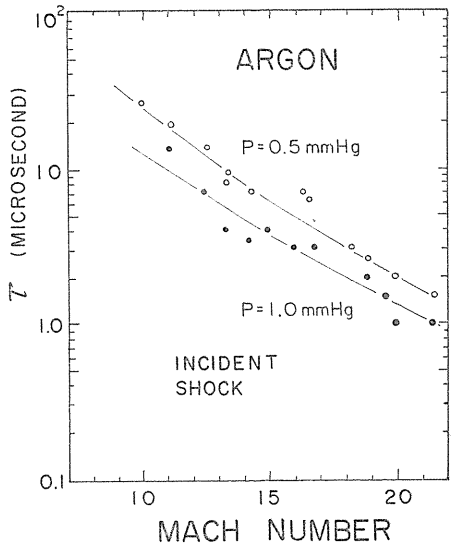

FIG. 11. Build-up time versus Mach number at different initial pressures.

to reach its maximum value from the luminous front, is plotted versus the Mach number in Fig. 11 for two different pressures in argon. This figure shows that the build-up time decreases, as the Mach number and the initial gas pressure increase. This shows the same tendency as that of the ionization time which is the time lag of the luminous front from the shock front.[29]

Figure 12 shows the radial distribution of the maximum electron density measured by the probe moving to the radial direction. R is the distance of the probe end from the shock tube axis. Since the resolution of the probe for the radial direction is approximately the penetration depth, the measured values are essentially local for the radial direction. It is seen that the maximum density behind the shock front is almost uniform except near the shock tube wall and that the uniformity becomes good with increasing Mach number. However, the maximum electron density near the wall is less by a factor of 2–5 than that near the center. This is due to the boundary layer at the wall. The boundary layer effect can be almost neglected for the probe whose end is about 5 mm from the wall.

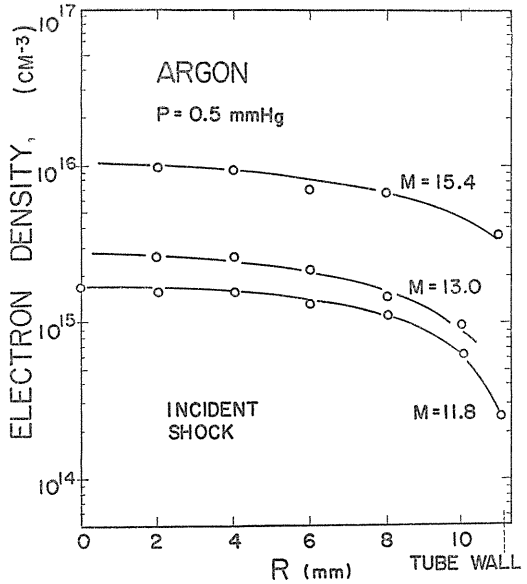

FIG. 12. Radial distributions of the maximum electron density for different Mach numbers.

(ii) Reflected shock waves

Measurements are made in hydrogen or helium. As an example, the result at $p=1.0$ mmHg in hydrogen is shown in Fig. 13. An excellent agreement is found between the electron densities measured with the microwave reflection probe and those from Stark broadening of the H_β line. Figure 14 shows the observed H_β profile which corresponds to the maximum electron density behind the reflected shock wave. Each point is the mean value of several shots. No correction is needed for spatial inhomogeneities of the plasma or for Doppler broadening and the instrumental width of the monochrometer. Both widths are less than 1 Å. The electron density n determined from the half-width of the profile in Fig. 14 is 1.1×10^{17} cm^{-3}. The electron temperature T_e determined from the ratio of total line intensities and the continuum intensity is 2.3×10^4 °K. This temperature does not contradict the temperature calculated from the electron density and collision frequency measured with the microwave reflection probe. The collision frequency of electrons with ions predominates over that with neutral atoms or molecules under the present experimental conditions.

In Table 1 are shown the maximum densities measured with the present

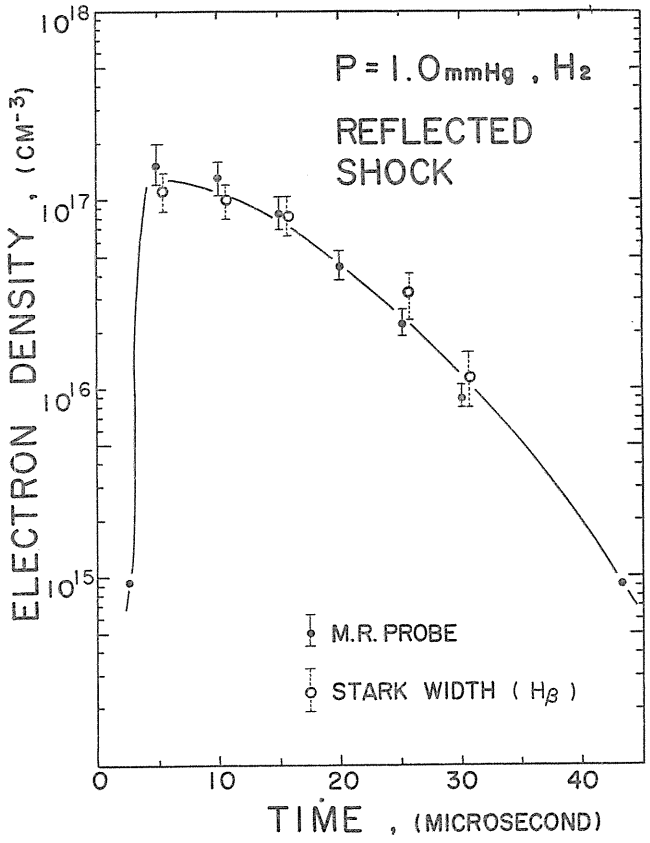

FIG. 13. Measured electron density behind the reflected shock wave.

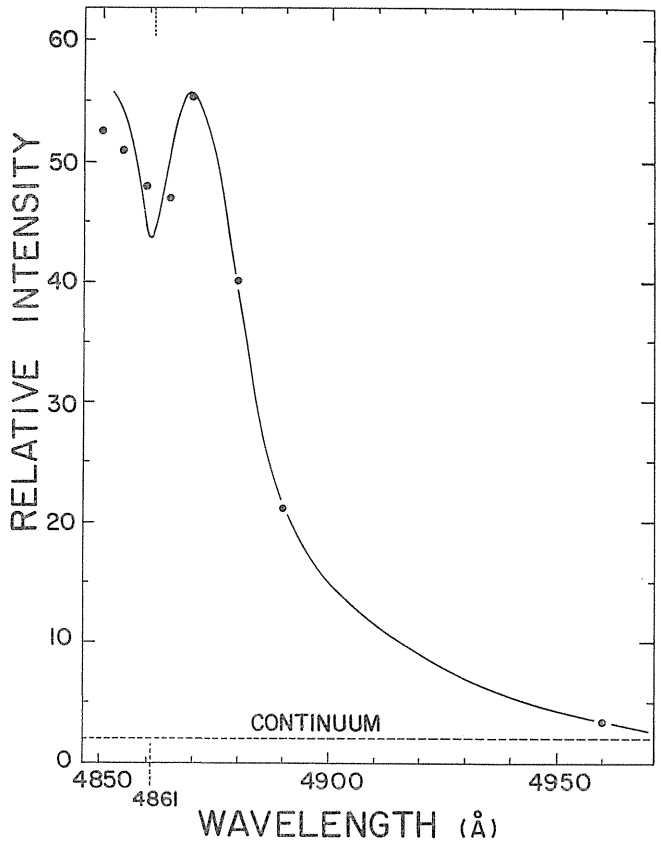

FIG. 14. Observed H_β profile ($n \simeq 1.1 \times 10^{17}$ cm^{-3}, $T_e \simeq 2.3 \times 10^{4}$°K).

TABLE 1. Comparisons of the maximum electron densities measured with the microwave reflection probe and from Stark broadening

	Initial pressure (mmHg)	Microwave reflection probe (cm^{-3})	Stark broadening (cm^{-3})
a H_2	1.0	$(1.5\pm0.4)\times10^{17}$	$(1.1\pm0.3)\times10^{17}$
b H_2	0.5	$(1.3\pm0.4)\times10^{17}$	$(1.0\pm0.2)\times10^{17}$
c H_2	2.0	$(4.5\pm0.9)\times10^{16}$	$(5.1\pm1.0)\times10^{16}$
d H_2	2.0	$(2.5\pm0.4)\times10^{16}$	$(1.9\pm0.6)\times10^{16}$
e H_e	2.0	$(4.8\pm1.0)\times10^{16}$	$(6.0\pm1.2)\times10^{16}$
f H_e	2.0	$(1.4\pm0.4)\times10^{17}$	$(1.5\pm0.3)\times10^{17}$

microwave reflection probe and from Stark broadening of the H_β or HeI (4471 Å). The satisfactory agreements indicate a reliability of the microwave reflection probe here described.

VI. Discussion

The measured maximum electron densities in Figs. 7, 8 and 9 are lower than the theoretically predicted values for lower Mach numbers, for example, by about a factor of 10 for $M\simeq 10$ and by a factor from 5 to 2 for $M\simeq 15$. The discrepancy becomes small with increasing initial pressure. It might be suspected that the present method does not show the real density because of perturbations by the probe. However, it is emphasized that the plasmas in reflected shock wave experiments are not disturbed, since the microwave reflection probe is positioned outside the shock tube. On the other hand, some of the electron densities measured by the probe inserted perpendicularly into the shock tube through its side wall are consistent with those of the other report[9]. The 35-Gc microwave cut-off, moreover, confirms one density value for a low Mach number. In addition, the electron densities measured from Stark broadening show no difference with and without the probe. This fact confirms a negligible probe disturbance in the density measurements, even though the disturbance on gas flow may be serious[30]. Both the measured and theoretical densities approach one another with increasing Mach number and agree well with each other for Mach numbers higher than 20. This result seems not to contradict earlier spectroscopic measurements[5]. In these works the agreement was found for $M\gtrsim 25$ between the experiment and the theory which was obtained from the Rankine-Hugoniot and Saha equations modified by the pre-excitation effect due to a radiative energy transfer from the initial arc discharge.

Under the present experimental conditions, the mean free path of the radiation from the initial arc discharge is, at most, a few centimeters in helium[5]. Thus the effect is expected to be small at the observation positions (50 or 67 cm away from the electrodes of the shock tube). The effect of the precursor radiation which originates in the plasma immediately behind a shock front will be also so small that it does not seem to affect drastically the hydrodynamic considerations and does not seem to explain the observed large discrepancy between the experiment and the theory for low Mach numbers. In addition, since these precursor effects become large with increasing shock strength, or with increasing Mach number, the precursors are not possible explanations of the observed discrepancy.

In the plasmas produced by shock waves of moderate strength ($n\lesssim 10^{17}$ cm^{-3}, $T\lesssim 2\times 10^{4}$°K), second ionization is very infrequent and the excitation energies of ion and neutral atom are usually very small compared with the other terms in the enthalpy equation. Thus, the approximation neglecting second ionization and the excitation energy in theoretical calculations is well justified under the present experimental conditions.

The most likely explanation of the observed discrepancy is the fact that the relaxation time effect behind a shock front is neglected in the theoretical considerations. During the ionization process behind the shock front, some loss processes such as the heat dissipation and the recombination of charged particles generally proceed. When the build-up time of the electron density is relatively long as shown for $M=11.1$ in Fig. 10, the loss effects are thought to be significant. In such cases, the electron density behind the shock front builds up at the rate which is determined from a competitive mechanism between the ionization and loss rates. The electron density takes on a final value which is less than the equilibrium value calculated by assuming that the various loss processes can be

neglected and that the thermal equilibrium can be established behind the shock front. Moreover, when a duration time of the plasma is not so long compared with the build-up time, the electron density attains only to a certain value much less than the equilibrium value. Thus the effect of the plasma duration perhaps influences remarkably the results in an electromagnetically driven shock tube, where the duration time is normally very short compared with a conventional pressure driven shock tube[1]. The long relaxation time effect will be an explanation of the observed discrepancy for low Mach numbers between the measured and theoretical densities.

On the other hand, at sufficiently high Mach numbers the relaxation time is very short and the ionization by collision processes dominates the losses. The build-up time (<1 μsec.) is much shorter than the plasma duration ($\sim$ the characteristic decay time, ~ 10 μsec.) for $M=21.7$ in Fig. 10. In this case, the thermal equilibrium is almost established and the electron densities agree well with the theoretically predicted values.

Since the build-up time is almost inversely proportional to the initial pressure and the rapidly decreasing function of the Mach number as is shown in Fig. 11, the discrepancy between the measured and theoretical values becomes large with decreasing Mach number and initial pressure. In addition, it is probable that the discrepancy is smaller behind reflected shock waves since the relaxation time is shorter and the duration time is longer than those behind propagating shock waves.

VII. Conclusion

The experiments show that the measured maximum electron densities produced by electromagnetically driven shock waves agree well with the theoretically predicted values from the simple hydrodynamic considerations for Mach numbers higher than 20, but does not for low Mach numbers. The discrepancy between the experiment and the theory for low Mach numbers is explained by considering the long relaxation time effect behind the shock front.

In spite of the relatively large probe inserted into the shock tube, surprisingly accurate measurements are obtained since the plasmas are not seriously disturbed by the probe. The measured electron density is in good agreement with other independent measurements for both high and low Mach numbers.

A satisfactory agreement between the electron densities measured with the present microwave reflection probe and those from Stark broadening also shows that the present method is quite reliable under some experimental conditions.

The authors wish to thank Dr. T. Tsukishima for his discussion and Dr. R. Taussig for his reading the manuscript with comments. The help by Mr. M. Kando in the latter part of the experiments is also appreciated.

Reference

1) A. C. Kolb and H. R. Griem, Atomic and Molecular Processes, edited by D. R. Dates (Academic Press, New York, 1962) p. 141.
R. A. Gross, Rev. Mod. Phys., **37**, 724 (1965).
2) F. L. Tevelow, J. Appl. Phys., **38**, 1765 (1967).

3) N. N. Sobolev *et al.*, Proceedings of V International Conference on Ionization Phenomena in Gases (Munich, 1961) vol. II 2122.
H. E. Petschek, P. H. Rose, H. S. Glick, A. Kane, and A. Kantrowitz, J. Appl. Phys., **25**, 83 (1955).
O. Laporte and T. D. Wilkerson, J. Opt. Soc. Amer., **50**, 1293 (1960).
4) H. F. Berg, A. W. Ali, R. Lincke, and H. R. Griem, Phys. Rev., **125**, 199 (1962).
R. C. Elton and H. R. Griem, Phys. Rev., **135**, A 1550 (1964).
5) E. A. McLean, C. E. Faneuff, A. C. Kolb, and H. R. Griem, Rhys. Fluids, **3**, 843 (1960).
W. Wiese, H. F. Berg, and H. R. Griem, Phys. Rev., **120**, 1079 (1960).
6) E. A. McLean and S. A. Ramsden, Phys. Rev., **140**, A 1122 (1965).
7) R. A. Alpher and D. R. White, Phys. Fluids, **2**, 153 (1959).
ibid., **2**, 162 (1959), *ibid.*, **4**, 40 (1961).
8) M. A. Heald and C. B. Wharton, Plasma Diagnostics with Microwaves (John Wiley and Sons Inc., New York, 1965).
9) T. I. McLaren, J. N. Fox, and R. M. Hobson, Proceedings of VI Internatinal Conference on Ionization Phenomena in Gases (Paris, 1963), vol. III, 311 (1963).
10) J. P. Barach and J. A. Sivinski, Phys. Fluids, **7**, 1075 (1964).
11) S. Takeda and M. Roux, J. Phys. Soc. Japan, **16**, 95 (1961).
12) T. Tsukishima and S. Takeda, J. Appl. Phys., **33**, 3290 (1962).
13) S. Takeda and T. Tsukishima, J. Phys. Soc. Japan, **21**, 426 (1963).
14) S. Takeda and T. Tsukishima, J. Appl. Phys., **35**, 2548 (1964); Proceedings of VI International Conference on Ionization Phenomena in Gases (Paris, 1963), vol. IV 177.
15) C. K. McLane, S. Takeda, W. E. Thomas, Jr., and R. C. Thompson, J. Appl. Phys., **36**, 337 (1965).
16) S. Takeda, T. Tsukishima, and A. Funahashi, Proceedings of VII International Conference on Ionization Phenomena in Gases (Belgrade, 1965), vol. II, 797.
17) R. A. Brandewie and E. M. Williams, J. Appl. Phys., **35**, 2299 (1964).
18) G. W. Bethke and A. D. Ruess, Phys. Fluids, **7**, 1446 (1964).
19) S. Takeda and A. Funahashi, Appl. Phys. Letters, **8**, 105 (1966).
20) S. Takeda and T. Tsukishima, NBS Technical note No. 256 (March, 1965), U. S. Department of Commerce, National Bureau of Standards.
21) S. Takeda and M. Masumi, Japan J. Appl. Phys., **5**, 1100 (1966).
22) This can be verified in the plane or guided wave propagation.
23) H. Hermansdorfer, Report of Institut für Plasmaphysik IPP 1/37 (1965).
24) E. L. Resler, S. C. Lin, and A. Kantrowitz, J. Appl. Phys., **23**, 1398 (1952).
25) S. C. Lin, R. A. Neal, and W. I. Fyfe, Phys. Fluids, **5**, 1633 (1962).
26) W. L. Wiese, Plasma Diagnostic Techniques, edited by R. H. Huddlestone and S. L. Leonard (Academic Press, New York 1965), p. 265.
H. R. Griem, Plasma Spectroscopy (McGraw-Hill Book Company, New York, 1964).
27) The Stark broadening is practically independent of the assumption of local thermal equilibrium.
28) C. T. Chang, Phys. Fluids, **4**, 1085 (1961),
M. Cloupeau, Phys. Fluids, **6**, 679 (1963).
29) V. H. Blackman and B. Niblett, The Plasma in a Magnetic Field, edited by R. K. M. Landshoff (Stanford University Press, Stanford, California, 1958) p. 94.
30) In order to suppress the disturbance on the gas flow, a wedge was used (see ref. 2 or 25). However, the effect on the plasma seems not to be obvious.